MULTISCALE MODEL. SIMUL.
Vol. 10, No. 3, pp. 1046–1058


# NUMERICAL STUDIES OF HOMOGENIZATION UNDER A FAST CELLULAR FLOW*

GAUTAM IYER† AND KONSTANTINOS C. ZYGALAKIS‡

**Abstract.** We consider a two dimensional particle diffusing in the presence of a fast cellular flow confined to a finite domain. If the flow amplitude $A$ is held fixed and the number of cells $L^2 \to \infty$, then the problem homogenizes; this has been well studied. Also well studied is the limit when $L$ is fixed and $A \to \infty$. In this case the solution averages along stream lines. The double limit as both the flow amplitude $A \to \infty$ and the number of cells $L^2 \to \infty$ was recently studied [G. Iyer et al., preprint, arXiv:1108.0074]; one observes a sharp transition between the homogenization and averaging regimes occurring at $A \approx L^4$. This paper numerically studies a few theoretically unresolved aspects of this problem when both $A$ and $L$ are large that were left open in [G. Iyer et al., preprint, arXiv:1108.0074] using the numerical method devised in [G. A. Pavliotis, A. M. Stewart, and K. C. Zygalakis, *J. Comput. Phys.*, 228 (2009), pp. 1030–1055]. Our treatment of the numerical method uses recent developments in the theory of modified equations for numerical integrators of stochastic differential equations [K. C. Zygalakis, *SIAM J. Sci. Comput.,* 33 (2001), pp. 102–130].

**Key words.** homogenization, averaging, backward error analysis, Monte Carlo methods

**AMS subject classifications.** 35B27, 70K65, 37M15, 60H35

**DOI.** 10.1137/120861308

## 1. Introduction.

**1.1. Physical motivation.** Understanding the transport properties of particles moving in fluid flows subject to molecular diffusion [9, 22] is a problem of widespread interest. To single out a few of the many applications, we mention atmosphere/ocean science [6, 33] and flows in heterogeneous porous media [20].

From the modeling point of view, the simplest model is one ignoring inertial effects. In this case, the equation of motion for the particle is given by the stochastic differential equation (SDE)

$$dX_t = v(X_t, t)\, dt + \sigma\, dW_t, \tag{1.1}$$

where $X_t \in \mathbb{R}^d$, $v(x,t)$ is the fluid velocity field, and $\sigma$ is the molecular diffusion. This is known as the passive tracer model. Different variants of this model are used in an application-specific context. In many cases modeling the noise in (1.1) as delta correlated in time might not be enough. For example, in ocean transport [3], the noise arises from the unresolved velocity scales, which are correlated in time. In other applications (e.g., rain initiation [8, 33]), one additionally has inertial effects which cannot be neglected.

**1.2. Cellular flows.** In order to make such problems amendable to mathematical analysis, the velocity field $v(x,t)$ is usually assumed to have a specific statistical or geometrical structure mimicking features of real fluid flows. In this paper we restrict our attention to fast, time independent, two dimensional cellular flows. Thus (1.1) becomes

$$dX = Av(X)\, dt + dW_t, \tag{1.2}$$

where $A > 0$ is the magnitude of the velocity (more precisely, $A$ is the Péclet number measuring the ratio between advection and diffusion), $W$ is a standard (two dimensional) Brownian motion, and $v$ is a divergence-free vector field with "cellular trajectories" and magnitude 1. A typical example of $v$ is given by

$$v(x) = \nabla^\perp H \stackrel{\text{def}}{=} \begin{pmatrix} -\partial_2 H \\ \partial_1 H \end{pmatrix}, \quad \text{where } H(x_1, x_2) \stackrel{\text{def}}{=} \frac{1}{2\pi} \sin(2\pi x_1)\, \sin(2\pi x_2). \tag{1.3}$$

For simplicity, we will subsequently assume that $v$ is given by (1.3). While the results we cite are usually valid in more general situations, the fact that $\Delta H = -4\pi H$ simplifies many of our calculations.

**1.3. Known results: Homogenization and averaging.** Equation (1.2) contains two natural nondimensional parameters: the number of cells, and the Péclet number. Homogenization studies the effective behavior of diffusive particles as the number of cells becomes large (and the Péclet number is held fixed). On long time scales the particle visits a large number of cells, and classical results [1, 17, 26] show that it effectively behaves like a rescaled Brownian motion. That is, for $t$ large, the law of $X_t$ is comparable to the law of $\sqrt{D_{\text{eff}}} W_t$, where $D_{\text{eff}}$, the effective diffusivity, is a constant matrix. The effective diffusivity can be obtained by solving a cell problem [5, 11], and asymptotic behavior as $A \to \infty$ is like $\sqrt{A} c_0 I$, where $I$ is the identity matrix and $c_0 > 0$ is a constant (see [11, 24, 35]).

In contrast, "averaging" studies the limiting behavior of the particle when the Péclet number $A$ becomes large (and the number of cells is held fixed). On short time scales when $A \to \infty$ the drift rapidly transports the passive tracer along level sets of $H$, and the noise slowly diffuses the tracer across level sets. This results in behavior that is averaged on level sets (more precisely, on the Reeb graph of the Hamiltonian), and this has been extensively studied by [12, 21] using the theory of large deviations and by [2, 30] using PDE methods.

Recently the transition between the averaged and homogenized behaviors was studied in [16] by confining the rapidly advected passive tracer confined to a large domain $\Omega$. The trajectories of $X$ (confined to $\Omega$) exhibit qualitatively different behavior, depending on the relative size of the Péclet number, $A$, to the number of cells in the domain, $L^2$. Theorem 1.3 in [16] shows that when $A \gg L^4$, trajectories of $X$ exit the domain immediately after reaching a cell boundary, forcing "ballistic" travel along separatrices. On the other hand, when $A \ll L^4$, the expected exit time of $X$ from $\Omega$ is comparable to that of the effective Brownian motion, suggesting that $X$ exhibits a homogenized behavior.

The different qualitative behavior observed in [16] is nicely illustrated in Figure 1. For a small Péclet number relative to the number of cells (precisely, $A = L = 10$), Figure 1(a) shows trajectories of $X$ resembling those of an effective Brownian motion. For a large Péclet number relative to the number of cells (precisely $A = L^{4.5}$, $L = 10$), Figure 1(b) shows multiple trajectories of $X$ which move "ballistically" along cell boundaries.

A heuristic explanation that the behavior of $X$ undergoes a transition at $A \approx L^4$ can be obtained by equating the expected exit times of the two regimes. If the flow

*Received by the editors January 4, 2012; accepted for publication (in revised form) June 4, 2012; published electronically September 13, 2012. This work was partially supported by the Center for Nonlinear Analysis (NSF DMS-0405343 and DMS-0635983) and NSF PIRE grant OISE 0967140.
http://www.siam.org/journals/mms/10-3/86130.html
†Department of Mathematical Sciences, Carnegie Mellon University, Pittsburgh, PA 15213 (gautam@math.cmu.edu). This author's research was partially supported by NSF-DMS 1007914.
‡School of Mathematics, University of Southampton, Southampton SO17 1BJ, UK (K.Zygalakis@soton.ac.uk). This author's research was partially supported by award KUK-C1-013-04 of the King Abdullah University of Science and Technology (KAUST). It was partially carried out at Carnegie Mellon University, whose hospitality is gratefully acknowledged.

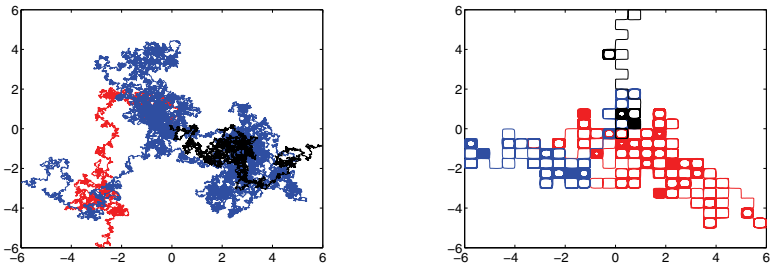

(a) Small amplitude (b) Large amplitude

FIG. 1. *Trajectories of three realizations of the diffusion* (1.2).

amplitude is weak, we expect that $X$ will behave like an effective Brownian motion with effective diffusivity $D_{\text{eff}} \approx \sqrt{A}I$. Thus, on average, $X$ should exit $\Omega$ in time $L^2/|D_{\text{eff}}| \approx L^2/\sqrt{A}$. On the other hand, if the flow amplitude is strong, then $X$ averages on level sets and diffuses across them. Thus the time $X$ takes to exit the entire domain should be comparable to the time $X$ takes to exit one cell, which is of order 1. Equating these two times, the behavior of $X$ should transition between regimes when $L^2/\sqrt{A} \approx 1$.

**1.4. Numerical results.** The aim of this paper is to numerically study the behavior of $X$ in the critical and homogenization regimes. In the averaging regime $A \gg L^4$, the asymptotic behavior of the expected exit time is rigorously obtained in [16]. However, in the homogenization regime $A \ll L^4$, only upper and lower bounds are obtained, and not an asymptotic profile. No results are obtained in the critical regime, and this paper numerically studies some of these issues.

**1.4.1. The critical regime.** The first question we numerically study is the critical case $A \approx L^4$. Our numerical observation was that a small fraction of trajectories travelled ballistically along separatrices and exited the domain almost immediately (see [34] for a related anomalous diffusion effect). Further, the remainder of nonballistic trajectories appear to behave exactly like those of an effective Brownian motion. Specifically, in section 3 we compare the distribution functions of the exit time of *nonballistic* trajectories to those of an effective Brownian motion and find a remarkable agreement. This seems to suggest that the behavior of $X$ in the critical regime can be decomposed into a very small ballistic component and a large homogenized component which behaves like an effective Brownian motion.

While the proportion of ballistic trajectories was significant enough to affect the comparison of density functions, it was too small to significantly affect the expected exit time. We numerically observed that the expected exit time of all (ballistic and nonballistic) trajectories of $X$ appeared identical to that of the effective Brownian motion.

The methods in [16] prove rigorous results in the cases $A \gg L^4$ and $A \ll L^4$ (with logarithmic corrections) but do not address the situation where $A \approx L^4$. Our numerics suggest that when $A \approx L^4$ the nonballistic trajectories might still exhibit a homogenized behavior.



**1.4.2. The homogenization regime.** The second question we numerically study is an issue left open in [16] when $A \ll L^4$. If we study the expected exit time of $X$ from a disk, then [16, Proposition 1.5] shows that as $A, L \to \infty$, the expected exit time converges to the expected exit time of an effective Brownian motion from the same disk. However, if we consider the expected exit time of $X$ from any other domain, then the results in [16] show that as $A, L \to \infty$, the expected exit time is only *comparable* to the expected exit time of an effective Brownian motion as $A, L \to \infty$. The failure to obtain an exact limit is a nontrivial obstruction stemming from extraneous terms in the asymptotic expansion. Our numerical simulations (presented in section 4) suggest that despite theoretical limitations, the expected exit time of $X$ from a square is exactly the expected exit time of the effective Brownian motion.

**1.4.3. Numerical method.** We mention here that the problem of simulating diffusion in cellular flows at high Péclet numbers has been studied before from a variety of authors. In particular, different PDE-based methods have been proposed in the literature, such as local mesh refinement [23], the unwinding method [18], and the stream-line diffusion method [7]. However, all these methods being PDE based, they aim to capture in one way or another the boundary layer, something that becomes increasingly difficult at higher Péclet numbers since then the methods become less stable.

Recently (see [13]) a combination of analytical and numerical techniques based on the asymptotic limit as the Péclet number approaches infinity was used. The use of exact asymptotics for the boundary layer [24] makes the performance of this method independent of the Péclet number.

In this paper, however, we follow a different approach by simulating individual stochastic trajectories with a carefully chosen stochastic integrator. This approach has the advantage that it does not require any specific knowledge of the boundary layer as in [13], while in addition, being a Monte Carlo method, it allows for the characterization of higher moments for the exit time $\tau$.

Finally, we comment on the choice of the stochastic integrator used for our simulations. Equation (1.2) is stiff, and when $A$ is large the standard Euler–Maruyama method requires a time step which is too small to be practically useful. We instead use the method developed in [28]. We conclude the paper with a description of the numerical method and a new, simpler analysis of it based on [36], which extends the theory of modified equations [32] to more general numerical integrators than the Euler–Maruyama method.

**1.5. Plan of this paper.** In section 2 we state a few results from [16] and provide a brief heuristic explanation. In section 3 we present our numerical results in the critical regime $A \approx L^4$. In section 4 we describe the issues in the homogenization regime $A \ll L^4$ that could not be addressed by the methods in [16] and present our numerical results. Finally, we conclude the paper with a description of the numerical method we used to perform our simulations.

**2. The homogenization and averaging regimes.** We devote this section to stating the results from [16] concerning the homogenization and averaging regimes. Let $\tau$ be the exit time of $X$ (defined in (1.2)) from the domain $\Omega$, and let $\bar{\tau}(x) \stackrel{\text{def}}{=} E^x\tau$ denote the expectation of $\tau$. It is well known (see, for instance, [25]) that the expected

exit time from the domain $\Omega$ satisfies the Poisson problem

$$\begin{cases} -\frac{1}{2}\Delta\bar{\tau} + Av\cdot\nabla\bar{\tau} = 1 & \text{in } \Omega, \\ \bar{\tau} = 0 & \text{on } \partial\Omega. \end{cases} \tag{2.1}$$

The results in [16] concern the limit of $\bar{\tau}$ and the principal eigenvalue of the operator $-\Delta + Av\cdot\nabla$ as both the Péclet number and the size of the domain $\Omega$ go to infinity. The result for the expected exit time (stated below) shows that the limit of $\bar{\tau}$ is either that of the homogenized equations or that of the averaged equations with a sharp transition at $A \approx L^4$.

THEOREM 2.1 (see [16]). *Let $\Omega = (-L/2, L/2)^2$ be a square of side length $L$, and let $\bar{\tau} = \bar{\tau}_{A,L}$ be the solution to (2.1):*

(a) *Suppose $L \to \infty$, and $A = A(L)$ varies so that $A \approx L^{4-\alpha}$ for some $\alpha \in (0,4)$. There exists a constant $C = C(\alpha) > 0$, independent of $A$ and $L$, such that*

$$\frac{1}{C}\frac{L^2}{\sqrt{A}}\bar{\tau}(x) \leqslant C\frac{L^2}{\sqrt{A}} \quad \text{whenever } |x| \leqslant (1-\delta)\frac{L}{2}. \tag{2.2}$$

*Consequently, as $L \to \infty$, we have $\bar{\tau} \to \infty$ uniformly on compact sets.*

(b) *On the other hand, suppose $A \to \infty$, and $L = L(A)$ varies so that $A \gg L^4$ (more precisely, we need $\sqrt{A}/(L^2 \log A \log L) \to \infty$). There exists a constant $C > 0$, independent of $A$ and $L$, such that*

$$\bar{\tau}(x)^2 \leqslant C\frac{L^2}{\sqrt{A}}\log A \log L \quad \text{whenever } H(x) = 0. \tag{2.3}$$

*Consequently, if $H(x) = 0$, then $\bar{\tau}(x) \to 0$ as $A \to \infty$, and $\|\bar{\tau}\|_{L^\infty(D)}$ is bounded uniformly in $A$.*

*Remark.* If $A$ is much smaller than $L$ (for instance, if $A$ is fixed and $L \to \infty$), then we expect homogenization to work. Thus, $X_t \approx \sqrt{D_{\text{eff}}}W_t$, and so we expect $\bar{\tau} \approx L^2/D_{\text{eff}} \approx L^2/\sqrt{A}$ away from $\partial\Omega$, which is exactly the content of (2.2).

*Remark.* If $A$ is much larger than $L$ (for instance, if $A \to \infty$ and $L$ is fixed), then we expect $X$ to behave like a diffusion averaged on level sets of $H$. Since both the boundary of the big domain $\Omega$ and the boundary of every cell are on the same level set of $H$, we expect the diffusion $X$ to exit immediately from cell boundaries. This is exactly (2.3) when $X$ starts on cell boundaries.

As mentioned earlier, equating the expected exit times from the homogenization and averaging regimes gives a quick heuristic explanation for why the transition occurs at $A \approx L^4$. We conclude this section with a very brief description of the ideas behind the proof of Theorem 2.1.

In the averaging regime ($A \gg L^4$), the central idea is to use an observation of Heinze [15], stating that

$$\|v\cdot\nabla\bar{\tau}\|^2_{L^2(\Omega)} \leqslant \frac{C}{A}\|\bar{\tau}\|_{L^1}.$$

Thus the convection forces $v\cdot\nabla\bar{\tau}$ to be small, and hence $\bar{\tau}$ cannot vary much along stream lines. Balancing this with the diffusion, which is responsible for the oscillation of $\bar{\tau}$ between neighboring cells, one can reduce the estimate for $\bar{\tau}$ to exit time estimate to a min-max combinatorial question. When $A \gg L^4$, the convection term dominates, and a cold boundary propagates inward along cell boundaries, all the way to the center cell. The techniques used are similar to those used in [10, 19], and the result itself (when $A \gg L^4$) can be deduced from [10].

When $A \ll L^4$, the estimate is much more delicate. The main idea is to use an asymptotic expansion, which surprisingly works only in the exceptional situation that the slow profile is quadratic! We describe this in more detail in section 4.



**3. Numerical results in the critical regime.** In this section we present our results for the exit time in the critical regime. We begin with Figure 2, a plot of $\bar{\tau}(L/2, L/2)$ versus $L$ for values of $L$ ranging from 10 to 80, with $A = L^4$ and the domain $\Omega$ being a square of side length $L$ (left) or a circle of diameter $L$ (right). The graph was computed using a Monte Carlo simulation using 10,000 realizations. The numerical method used is based on [28, 29] and is described in section 5.

To see that the mean exit time agrees with that of the homogenized process, we recall that the asymptotic behavior of the effective diffusion matrix is

$$D_{\text{eff}} = D_{\text{eff}}(A) \stackrel{\text{def}}{=} \lim_{t\to\infty}\frac{EX_t \otimes X_t}{t} \approx c_0\sqrt{A}\,I,$$

and we numerically compute $c_0 \approx 0.6056$. Now, the expected exit time of the homogenized process $\sqrt{D_{\text{eff}}}W$ from the center of a circle of diameter $L = A^{1/4}$ can be (analytically) computed to be $1/(8c_0) \approx 0.2064$, which agrees well with Figure 2(b). For the square of side length $L$, a numerical simulation shows that the expected exit time of $\sqrt{D_{\text{eff}}}W$ from the center is $0.1473/c_0 \approx 0.2433$, which agrees well with Figure 2(a).

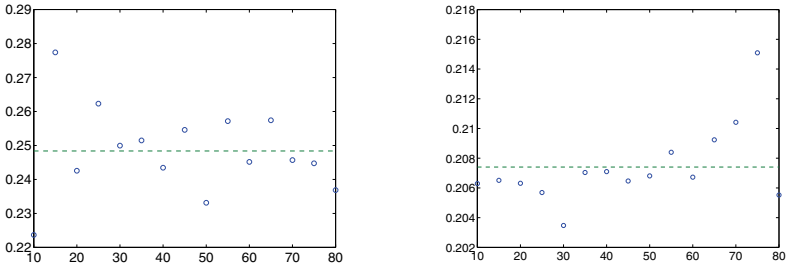


(a) Square of side length $L$ (b) Circle of diameter $L$

FIG. 2. *Expected exit time of $X$ for different values of $L$, with $A = L^4$.*

We now fix $L = 40$, $A = L^4$ and consider the exit time $\tau$ of the process $X$ from the center of a square of side length $L$ and a circle of diameter $L$. We observe that with small probability, some trajectories of $X$ will travel ballistically along separatrices and exit the domain very quickly. To study the nonballistic trajectories, we ignore all trajectories of $X$ that exit the domain in time less than a small time threshold (roughly 0.03 seconds). For the remaining trajectories, we compare the distribution $\tau$ to $\tau_{\text{eff}}$, the exit time of the effective Brownian motion $\sqrt{D_{\text{eff}}}W$. Our results show that the distributions are almost identical, and they are illustrated in Figure 3. Specifically, Figure 3(a) shows the cumulative distribution functions (CDFs) of $\tau$ and $\tau_{\text{eff}}$ from a square of side length 40, and Figure 3(b) shows the CDFs of $\tau$ and $\tau_{\text{eff}}$ from a circle of diameter 40.

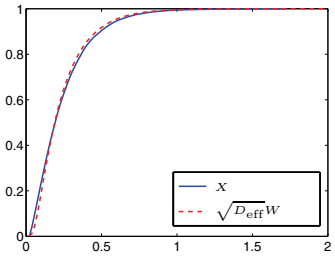


(a) Square of side length 40

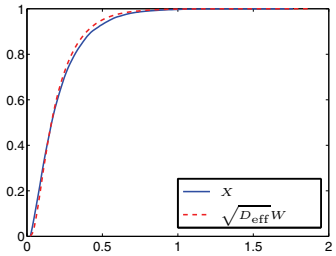


(b) Circle of diameter 40

FIG. 3. *CDF for $\tau$ compared with the CDF of the exit time of the effective Brownian motion.*

**4. Numerical results in the homogenization regime.** A fundamental question left unresolved by [16] is about the asymptotic profile of $\bar{\tau}$ in any domain which is not a disk. This roughly translates to the question of whether "homogenization works" when the asymptotic profile is not quadratic. We explain the theoretical obstruction and our numerical findings in this section.

The proof of Theorem 2.1 in the homogenization regime (i.e., $A \ll L^4$) uses an asymptotic expansion. To carry this out, we rescale the domain to a square of side length 1 which we denote by $\Omega_1$. Let $\varepsilon = 1/L$, and let $\bar{\sigma} = \bar{\sigma}_{A,\varepsilon}$ be the rescaled function defined by $\bar{\sigma}(x) = \varepsilon^2 \bar{\tau}(x/\varepsilon)$. Then, $\bar{\sigma}$ satisfies the equation

$$\begin{cases} -\frac{1}{2}\Delta\bar{\sigma} + \frac{A}{\varepsilon} v\left(\frac{x}{\varepsilon}\right) \cdot \nabla\bar{\sigma} = 1 & \text{in } \Omega_1 \overset{\text{def}}{=} (0,1)^2, \\ \bar{\sigma} = 0 & \text{on } \partial\Omega_1. \end{cases} \tag{4.1}$$

Now consider a multiscale expansion of an approximate solution $\tilde{\sigma}$ up to two terms:

$$\tilde{\sigma}(x) = \sigma_0(x) + \varepsilon\sigma_1(x,y) + \varepsilon^2\sigma_2(x,y), \quad \text{where } y = \frac{x}{\varepsilon} \text{ is the "fast" variable.}$$

The usual practice in homogenization [1, 26] is to choose $\sigma_0$ to be a solution of the effective problem and then choose $\sigma_1, \sigma_2$ to be functions which are periodic and mean zero in the fast variable, and satisfy equations that balance the $O(\varepsilon)$ and $O(1)$ terms, respectively.

While this works perfectly well for $A$ fixed, the proofs in [16] will only work in an *exceptional situation* if $A \to \infty$. To elaborate on this, choosing $\sigma_1$, $\sigma_2$ as described above, we will obtain

$$\begin{aligned} -\frac{1}{2}\Delta\tilde{\sigma} + \frac{A}{\varepsilon} v\left(\frac{x}{\varepsilon}\right) \cdot \nabla\tilde{\sigma} = -\Delta\left(\sigma_0 + \varepsilon\sigma_1 + \varepsilon^2\sigma_2\right) \\ + A\langle v \cdot \nabla_x\sigma_1\rangle - 2\varepsilon\nabla_x \cdot \nabla_y\sigma_2 + \varepsilon A v \cdot \nabla_x\sigma_2, \end{aligned}$$

where $\langle\cdot\rangle$ denotes the average with respect to the fast variable. When $A$ is fixed, all terms with an $\varepsilon$ are harmless, and the term $A\langle v\cdot\nabla_x\sigma_1\rangle$ can be computed explicitly [11, 24]. When we additionally have $A \to \infty$, the presence of the term $\varepsilon A v \cdot \nabla_x\sigma_2$ is catastrophic! Fortunately this term *identically vanishes* in the exceptional situation that $\sigma_0$ is quadratic. It is this exceptional situation that [16] heavily exploits in the proof.



Observe that if one replaces $\Omega_1$ with $B(0,1)$ in (4.1), then $\sigma_0$ must be quadratic (explicitly, $\sigma_0 = \frac{1}{2\,\text{tr}(D_{\text{eff}}(A))}(1-|x|^2)$, where $D_{\text{eff}}(A)$ is the effective diffusivity matrix). In this case, the result in (2.2) can be improved considerably. For convenience, we state the improved result in rescaled coordinates.

THEOREM 4.1 (see [16]). *Suppose $\bar{\sigma}'$ is the solution to (4.1) on $B(0,1)$, the disk of radius 1. Suppose, for some $\alpha > 0$, $A = O(1/\varepsilon^{4-\alpha})$ as $\varepsilon \to 0$. Then there exists $c = c(\alpha) > 0$, independent of $A, \varepsilon$, such that for all $\varepsilon$ sufficiently small,*

$$\|\bar{\sigma} - \sigma_0\|_{L^\infty} \leqslant c\frac{\varepsilon}{A^{1/4}}, \tag{4.2}$$

*where $\sigma_0 = \sigma_0(A)$ is the solution of the effective problem*

$$-\nabla \cdot D_{\mathit{eff}}(A)\nabla\sigma_0 = 1 \quad \textit{in } B(0,1) \qquad \textit{and} \qquad \sigma_0 = 0 \quad \textit{on } \partial B(0,1).$$

Observe that $D_{\text{eff}}(A) = O(\sqrt{A})$, and hence $\sigma_0 = O(1/\sqrt{A}) \to 0$; however, the right-hand side of (4.2) is $\varepsilon/A^{1/4} = o(1/\sqrt{A})$ by assumption. This means that the limiting profile of $\sqrt{A}\bar{\sigma}$ is exactly $\sqrt{A}\sigma_0$, which is finite and nonzero in the interior of $B(0,1)$. On the other hand, (2.2) provides only upper and lower bounds for the limiting profile of $\bar{\sigma}$.

We numerically confirm that (4.2) is valid in a situation where $\sigma_0$ is not quadratic. For this, we return to studying the (rescaled) expected exit time $\bar{\sigma}$ on $\Omega_1$, the square of side length 1. Figure 4(a) shows slices of the graphs of $\bar{\sigma}$ and $\sigma_0$ along the diagonal of the square $\Omega_1$. Figure 4(b) shows slices of the graphs of $\bar{\sigma}$ and $\sigma_0$ along a horizontal line through the center. Figures 4(c) and 4(d) show the same slices on a $1.5 \times 2.5$ rectangle, instead of the square $\Omega_1$. We observe a remarkable agreement between $\bar{\sigma}$ and $\bar{\tau}_0$, suggesting that (4.2) is valid for general $\sigma_0$, despite apparent theoretical obstacles arising from the catastrophic $\varepsilon A v \cdot \nabla_x\sigma_2$ term.

**5. Numerical method.** We conclude this paper with a description of the numerical method used for our simulations. As mentioned earlier, the Euler–Maruyama method is not suitable for our purposes, and the method we use is that in [28]. We describe the method here and present a simplified analysis of it based on the theory of modified equations.

We first rescale time by a factor of $1/A$ and consider the process $Y_t \overset{\text{def}}{=} X_{t/A}$. With this change, SDE (1.2) becomes

$$dY_t = v(Y_t)\,dt + \frac{1}{\sqrt{A}}\,dW'_t, \tag{5.1}$$

where $W'_t = \sqrt{A}W_{t/A}$ is a new Brownian motion.

Observe that for large $A$, the SDE (5.1) is a small random perturbation of the Hamiltonian system

$$\frac{dY}{dt} = v(Y), \tag{5.2}$$

with Hamiltonian $H$ (see (1.3)). So it is natural to look for numerical schemes which respect features of the underlying deterministic dynamics [14]. The scheme we use is based on the (deterministic) scheme in [29].

Define $d_i, e_i$ by

$$d_1 = \begin{pmatrix} -1/2 \\ 1/2 \end{pmatrix}, \quad d_2 = \begin{pmatrix} -1/2 \\ -1/2 \end{pmatrix}, \quad e_1 = 2\pi\begin{pmatrix} 1 \\ 1 \end{pmatrix}, \quad e_2 = 2\pi\begin{pmatrix} 1 \\ -1 \end{pmatrix}, \tag{5.3}$$

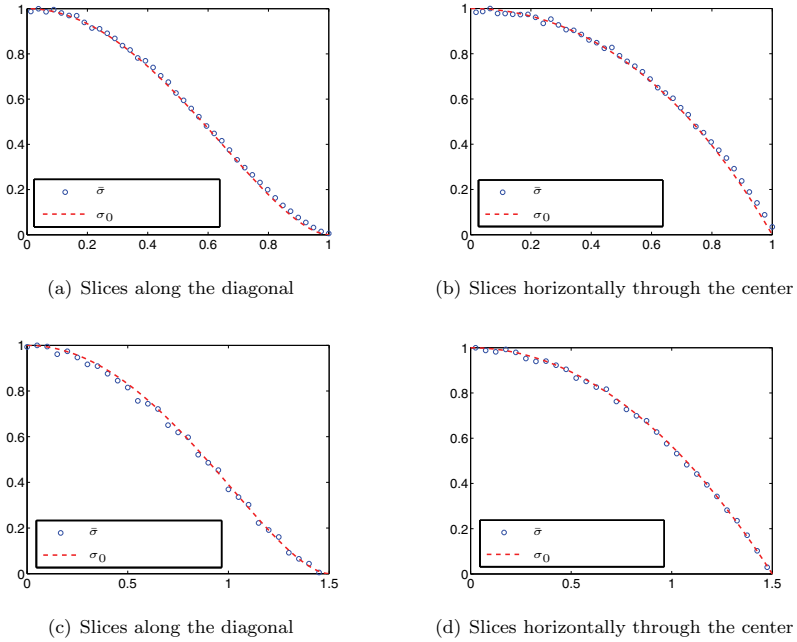


(a) Slices along the diagonal (b) Slices horizontally through the center

(c) Slices along the diagonal (d) Slices horizontally through the center

FIG. 4. *Slices of the graphs of $\bar{\sigma}$ and $\sigma_0$ in a square (top) and rectangle (bottom).*

and observe that

$$v = \sum_{i=1}^{2} v_i, \quad \text{where } v_i(x) = d_i g(\langle e_i, x\rangle), \text{ and } g(x) = \sin(x).$$

Here $\langle\cdot,\cdot\rangle$ denotes the standard inner product on $\mathbb{R}^2$.

The main idea behind the scheme in [29] is that each constituent vector field $v_i$ is divergence-free and can be integrated explicitly. Namely, in view of the identities,

$$\langle d_i, e_i\rangle = \langle d_i, d_j\rangle = \langle e_i, e_j\rangle = 0 \quad \text{for } i,j \in \{1,2\}, \text{ with } i \neq j,$$

we see that

$$\begin{aligned} &\dot{Z}_t(z) = v_i(Z_t(z)), \\ &Z_0(z) = z \end{aligned} \qquad \Longleftrightarrow \qquad Z_t(z) = z + t d_i g(\langle e_i, z\rangle). \tag{5.4}$$

In view of (5.4), using the Euler method to integrate each constituent field $v_i$ will give an explicit, *volume preserving*, numerical integrator for $v$. Of course, volume preserving integrators cannot also preserve the Hamiltonian unless they coincide with the exact flow [4]. However, this numerical method preserves a modified Hamiltonian (discussed later), preventing it from "spiralling outward," which is usually the difficulty encountered when the Euler method is used to integrate (5.2) over long time intervals. In particular, it is possible to show that the application of the Euler method to an ODE of the form (5.2) results in a drift of the Hamiltonian, the rate of which is



proportional to the time step $\Delta t$, leading in the case of our problem[1] to trajectories spiralling outward, as observed in [28].

In the stochastic setting, we choose a sequence of independent random variables $(\xi_n)$ so that each $\xi_n$ is a two dimensional normally distributed random variable with mean 0 and covariance matrix $I$. Let $\Delta t > 0$ be the time step, and let $y \in \mathbb{R}^2$ be the initial condition. We define $Y^n$, an approximation to the solution of (5.1) at time $n\,\Delta t$, by

$$\begin{cases} Z_1^n = Y^n + \Delta t\, d_1 g(\langle Y^n, e_1\rangle), \qquad Z_2^n = Z_1^n + \Delta t\, d_2 g(\langle Z_1^n, e_2\rangle), \\ Y^{n+1} = Z_2^n + \left(\dfrac{\Delta t}{A}\right)^{1/2} \xi_n, \end{cases} \tag{5.5}$$

with $Y^0 = y$. It quickly follows from (5.4) that the map $y \mapsto Y^n$ is (surely) volume preserving for all $n$. Thus (5.5) gives us a volume preserving numerical scheme for (5.1) whose inviscid counterpart does not spiral outward!

We remark here on the applicability of our method to more complicated flows. The original method, proposed in the deterministic setting in [29], deals with source-free vector fields that are polynomial functions of trigonometric functions of the field variables. This work was extended in [28] for velocity fields for the type considered in [29], for equations of the form (1.2), and for the case of inertial particles. Thus as long as we have a divergent velocity field which can be written as a sum of trigonometric polynomials we can always apply our method. This, of course, would not be the case for more general Hamiltonians; however, the philosophy behind the choice of the numerical method should be the same, namely to use a numerical method that in the absence of noise is appropriate for the long time integration of Hamiltonian systems [14].

**5.1. An analysis of the method using modified equations.** A simple analysis of the qualitative features of our numerical scheme can be obtained using the theory of modified equations for SDEs [32, 36]. In particular, assume that (5.1) is solved by a first order weak method, such as, for example, the stochastic splitting method (5.5). Then one looks for coefficients $u_1(x), \sigma_1(x)$ such that (5.5) approximates

$$dY_t = [u(Y_t) + \Delta t u_1(Y_t)]\, dt + \left[\frac{1}{\sqrt{A}} + \Delta t \sigma_1(Y_t)\right] dW_t \tag{5.6}$$

weakly to second order. The coefficients $u_1, \sigma_1$ can be calculated following [32] when the numerical method used is the Euler–Maruyama method. For more complicated numerical integrators a more general framework is developed in [36].

The underlying idea for calculating these coefficients is that $u_1, \sigma_1$ should be chosen such that the "modified" local error between the numerical method and the solution of (5.6) should be one order higher than the "original" local error between the numerical method and the solution of (5.1). This is accomplished primarily using weak stochastic Taylor expansions [31]. In our situation, $u_1$ and $\sigma_1$ can be calculated using equation (3.9) in [36], which shows that (5.5) approximates

$$dY_t = \nabla^\perp \tilde{H}(Y_t)\, dt + \frac{1}{\sqrt{A}}\left(I - \frac{\Delta t}{2}\nabla v(Y_t)\right) dW_t \tag{5.7}$$

[1] For a more general discussion see [14].

weakly to second order. Here $v$ is our velocity field from (1.3), and $\tilde{H}$ is the modified Hamiltonian defined by

$$\tilde{H} = H(x)\left(1 + \frac{2\pi^2\Delta t}{A}\right) + \Delta t H_1(x), \tag{5.8}$$

where

$$H_1(x_1, x_2) = \frac{1}{16\pi^2}\left(\cos 4\pi x_2 - \cos 4\pi x_1\right). \tag{5.9}$$

Observe that the modified equation (5.7) is a random perturbation of a two dimensional Hamiltonian flow with a cellular Hamiltonian $\tilde{H}$. It is easy to see that as long as $\Delta t = o(1)$, solutions to (5.7) approximate solutions to (5.1). Consequently, this means that our method will integrate (1.2) on the time interval $[0, 1]$ in roughly $A$ steps. The Euler–Maruyama method, in contrast, will require roughly $A^2$ steps. Finally, we remark that when comparing the modified equation (5.7) with that obtained from the deterministic analysis [14], the only extra term that appears in $\tilde{H}$ is $\frac{2\pi^2\Delta t}{A}H$, which accounts for the presence of noise in the problem. We point out here that this analysis would still be applicable in the case of more complicated two dimensional flows; however, in this case it greatly simplifies due to the fact that $\Delta H = -4\pi H$.

**6. Conclusions and some open problems.** Our first numerical observation was that in the critical regime, the trajectories of $X$ appear to be divided into two separate groups: a very small ballistic component, and a large homogenized component. A rigorous result proving this effect, or even for the expected behavior, is open. Further, as our numerics involve the exit time, we directly see that the trajectories of $X$ are not "stuck" at degenerate critical points of $H$ (the cell corners).

Our second numerical observation suggests that in the homogenization regime ($A \ll L^4$), the spatial dependence of the exit time $\bar{\tau}$ converges to that of an effective Brownian motion. Rigorous analytical results only prove convergence when the domain is a disk! In any other domain, only upper and lower bounds are known, but a rigorous result proving convergence is open.

Finally, from both the numerical and theoretical points of view a very challenging problem is the one of inertial particles. In this case homogenization results still hold for periodic velocity fields [27], but nothing is known analytically about the exact asymptotic behavior of the effective diffusivity in the limit of zero diffusivity. Numerical simulations [28] indicate a highly nonlinear behavior for it in this limit, making the study of exit time problems similar to that considered here a very challenging problem.

## REFERENCES


[1] A. Bensoussan, J.-L. Lions, and G. Papanicolaou, *Asymptotic Analysis for Periodic Structures*, Stud. Math. Appl. 5, North–Holland, Amsterdam, 1978.

[2] H. Berestycki, F. Hamel, and N. Nadirashvili, *Elliptic eigenvalue problems with large drift and applications to nonlinear propagation phenomena*, Comm. Math. Phys., 253 (2005), pp. 451–480.

[3] P. Castiglione and A. Crisanti, *Dispersion of passive tracers in a velocity field with non-δ-correlated noise*, Phys. Rev. E (3), 59 (1999), pp. 3926–3934.

[4] P. Chartier, E. Faou, and A. Murua, *An algebraic approach to invariant preserving integrators: The case of quadratic and Hamiltonian invariants*, Numer. Math., 103 (2006), pp. 575–590.





[5] S. Childress, *Alpha-effect in flux ropes and sheets*, Phys. Earth Planet Inter., 20 (1979), pp. 172–180.

[6] G. T. Csanady, ed., *Turbulent Diffusion in the Environment*, Vol. 3, D. Reidel, Dordrecht, The Netherlands, 1973.

[7] J. Douglas, Jr., and T. F. Russell, *Numerical methods for convection-dominated diffusion problems based on combining the method of characteristics with finite element or finite difference procedures*, SIAM J. Numer. Anal., 19 (1982), pp. 871–885.

[8] G. Falkovich, A. Fouxon, and M. G. Stepanov, *Acceleration of rain initiation by cloud turbulence*, Nature, 419 (2002), pp. 151–154.

[9] G. Falkovich, K. Gawedzki, and M. Vergassola, *Particles and fields in fluid turbulence*, Rev. Modern Phys., 73 (2001), pp. 913–975.

[10] A. Fannjiang, A. Kiselev, and L. Ryzhik, *Quenching of reaction by cellular flows*, Geom. Funct. Anal., 16 (2006), pp. 40–69.

[11] A. Fannjiang and G. Papanicolaou, *Convection enhanced diffusion for periodic flows*, SIAM J. Appl. Math., 54 (1994), pp. 333–408.

[12] M. I. Freidlin and A. D. Wentzell, *Random Perturbations of Dynamical Systems*, 2nd ed., Grundlehren Math. Wisse. 260, Springer-Verlag, New York, 1998.

[13] Y. Gorb, D. Nam, and A. Novikov, *Numerical simulations of diffusion in cellular flows at high Péclet numbers*, Discrete Contin. Dyn. Syst. Ser. B, 15 (2011), pp. 75–92.

[14] E. Hairer, C. Lubich, and G. Wanner, *Geometric Numerical Integration: Structure-Preserving Algorithms for Ordinary Differential Equations*, 2nd ed., Springer Ser. Comput. Math. 31, Springer-Verlag, Berlin, 2006.

[15] S. Heinze, *Diffusion-advection in cellular flows with large Peclet numbers*, Arch. Ration. Mech. Anal., 168 (2003), pp. 329–342.

[16] G. Iyer, T. Komorowski, A. Novikov, and L. Ryzhik, *From homogenization to averaging in cellular flows*, preprint, arXiv:1108.0074.

[17] V. V. Jikov, S. M. Kozlov, and O. A. Oleĭnik, *Homogenization of Differential Operators and Integral Functionals*, Springer-Verlag, Berlin, 1994.

[18] R. B. Kellogg and A. Tsan, *Analysis of some difference approximations for a singular perturbation problem without turning points*, Math. Comp., 32 (1978), pp. 1025–1039.

[19] A. Kiselev and L. Ryzhik, *Enhancement of the traveling front speeds in reaction-diffusion equations with advection*, Ann. Inst. H. Poincaré Anal. Non Linéaire, 18 (2001), pp. 309–358.

[20] D. L. Koch, R. G. Cox, H. Brenner, and J. F. Brady, *The effect of order on dispersion in porous media*, J. Fluid Mech., 200 (1989), pp. 173–188.

[21] L. Koralov, *Random perturbations of 2-dimensional Hamiltonian flows*, Probab. Theory Related Fields, 129 (2004), pp. 37–62.

[22] A. J. Majda and P. R. Krammer, *Simplified models for turbulent diffusion: Theory, numerical modeling, and physical phenomena*, Phys. Rep., 314 (1999), pp. 237–574.

[23] J. J. H. Miller, E. O'Riordan, and G. I. Shishkin, *Fitted Numerical Methods for Singular Perturbation Problems: Error Estimates in the Maximum Norm for Linear Problems in One and Two Dimensions*, World Scientific, River Edge, NJ, 1996.

[24] A. Novikov, G. Papanicolaou, and L. Ryzhik, *Boundary layers for cellular flows at high Péclet numbers*, Comm. Pure Appl. Math., 58 (2005), pp. 867–922.

[25] B. Øksendal, *Stochastic Differential Equations: An Introduction with Applications*, 6th ed., Universitext, Springer-Verlag, Berlin, 2003.

[26] G. A. Pavliotis and A. M. Stuart, *Multiscale Methods: Averaging and Homogenization*, Texts Appl. Math. 53, Springer, New York, 2008.

[27] G. A. Pavliotis and A. M. Stuart, *Periodic homogenization for inertial particles*, Phys. D, 204 (2005), pp. 161–187.

[28] G. A. Pavliotis, A. M. Stuart, and K. C. Zygalakis, *Calculating effective diffusiveness in the limit of vanishing molecular diffusion*, J. Comput. Phys., 228 (2009), pp. 1030–1055.

[29] G. R. W. Quispel and D. I. McLaren, *Explicit volume-preserving and symplectic integrators for trigonometric polynomial flows*, J. Comput. Phys., 186 (2003), pp. 308–316.

[30] P. B. Rhines and W. R. Young, *How rapidly is passive scalar mixed within closed streamlines?*, J. Fluid Mech., 133 (1983), pp. 135–145.

[31] A. Rössler, *Stochastic Taylor expansions for the expectation of functionals of diffusion processes*, Stoch. Anal. Appl., 22 (2004), pp. 1553–1576.

[32] T. Shardlow, *Modified equations for stochastic differential equations*, BIT, 46 (2006), pp. 111–125.

[33] R. A. Shaw, *Particle-turbulence interactions in atmosphere clouds*, in Annual Review of Fluid Mechanics, Annu. Rev. Fluid Mech. 35, Annual Reviews, Palo Alto, CA, 2003, pp. 183–227.

[34] W. Young, A. Pumir, and Y. Pomeau, *Anomalous diffusion of tracer in convection rolls*, Phys. Fluids A, 1 (1989), pp. 462–469.
[35] A. Zlatoš, *Reaction-diffusion front speed enhancement by flows*, Ann. Inst. H. Poincaré Anal. Non Linéaire, 28 (2011), pp. 711–726.
[36] K. C. Zygalakis, *On the existence and the applications of modified equations for stochastic differential equations*, SIAM J. Sci. Comput., 33 (2011), pp. 102–130.